

An Alternative Theory of Simple Pendulum Libration

Bradley Klee^{*}

Department of Physics, University of Arkansas, Fayetteville, AR 72701

(Dated: November 16, 2019)

Abstract

Integration along the transcendental Hamiltonian function $\alpha = 2H(p, q) = p^2 + \sin(q)^2$ predicts the time dependence of simple pendulum libration when $\alpha \in (0, 1)$. By equivalence via canonical transformation, the same can be said for the algebraic Hamiltonian function,

$$\alpha = 2H(p, q) = \left(p^2 + q^2\right)\left(1 - \frac{1}{4}q^2\right),$$

a close relative to Harold Edwards's normal form for elliptic curves. Combining real and complex transformation theory with Edwards's theory of elliptic curves and elliptic functions, we derive an exact solution of the simple pendulum's librational equations of motion.

^{*} bjklee@email.uark.edu, bradklee@gmail.com

I. HISTORY AND INTRODUCTION

The universal law of gravitation¹ guarantees an analogy between the libration of a pendulum around its fixed axis and the orbital motion of a planet around its central star. The entire analogy goes deeper than to simply describe a planet and a pendulum bob as massive objects affected by gravitational forces. In both cases, the equations of motion have oscillating solutions, which return to their initial conditions after a fixed interval of time. In both cases, the recurrence periods depend on an amplitude parameter that enters through the initial conditions. Here the analogy reveals its great fallacy. The two period functions do not share very many similarities, nor are they equally difficult to solve or to measure. The discovery and resolution of this dichotomy plays across many interesting chapters from the history of science, and leads into the subject matter of this current work.

About a century before the advent of integral calculus, Galileo (1564-1642) made the simple observation that two pendulums of the same characteristic length will undergo isochronous oscillations. The observation does not hold true outside the small angle limit, as Galileo may very well have known². A counterpoint to this story occurs in the researches of Kepler (1571-1630), who first discovered the three laws of planetary motion. The third law asserts that the square of a planet's yearly period is proportional to the cube of the orbital ellipse's semi-major axis length. In a sense, Kepler succeeded where Galileo could not. He was able to correctly ascertain the functional dependence of an oscillation period. Meanwhile, significant obstacles in theory and experiment stood between renaissance scientists and a better understanding of pendulum dynamics.

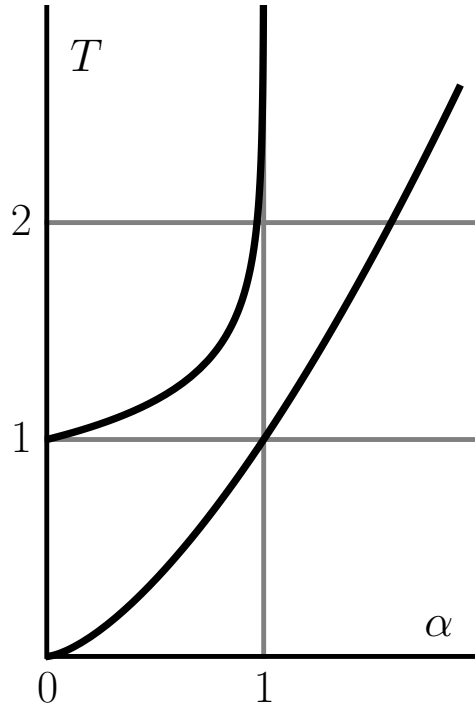


FIG. 1. Two period functions.

¹ For an introduction, try *Feynman Lectures on Physics*, Vol. I, Ch. 7 [1].

² As Bill Gosper speculates in an email from Sunday July 7, 2019, 05:33:49 UTC.

Though the planets can not be controlled in a laboratory as can a pendulum bob, the planetary period function is sometimes easier to measure than that of a simple pendulum³. Using only XVI century implements, an astronomer can chart the day-to-day motion of a planet at a resolution of tens or hundreds of data points per yearly cycle. Without digital acquisition of data, a similar sampling of pendulum motion at 10 to 100 Hertz is practically impossible. Dissipative losses introduce uncertainty to measured values and compound upon difficulties due to short timescale. Even if renaissance experimental scientists could have accurately measured changes of the pendulum's period on the order of a few percents, the analytic task of extracting a functional form would have been an impossible prospect before the theoretical advances of Euler (1707-1783). The period function in question is not algebraic, nor is it immediately easy to characterize by fitting only a few free parameters.

Among hundreds of other topics, Euler initiated the general study of elliptic integrals and hypergeometric series, and subsequently solved exactly for the simple pendulum's amplitude dependence⁴. Careful examination of publication records reveals yet another example of Arnold's principle that "discoveries are rarely attributed to the correct person". Euler could already understand the hypergeometric function ${}_2F_1(a, b; c; z)$ in terms of its characteristic differential equation,

$$a b F - (c - (a + b + 1)z) \partial_z F - z(1 - z) \partial_z^2 F = 0,$$

yet most authors credit the later Gauss (1777-1855), who gave a more extensive treatment and standardized notation, decades after Euler's exploratory work [4]. In any case, the hypergeometric function eventually came to be seen as a crown accomplishment of classical function theory and a *sine qua non* of period analysis [5].

Up to a scale degree of freedom or an initial value, the two ordinary differential equations,

$$3 T - 2 \alpha \partial_\alpha T = 0 \quad \text{vs.} \quad T - \partial_\alpha (4 \alpha (1 - \alpha) \partial_\alpha T) = 0,$$

define the periods of planetary and pendulum motion respectively, as seen in Figure 1. Integers 2 and 3 appearing in the first equation are the exponents already known to Kepler. Integer 4 appearing in the second equation is not so easy to explain. Choosing hypergeometric

³ For a popular discussion of Galileo, Kepler, and early measurements, try *Infinite Powers* [2].

⁴ Cf. Euler Archive [3]: E028, E366, E503.

parameters $(a, b, c) = (1/s, (s-1)/s, 1)$, the general equation reduces to a factored form,

$$(s-1)F - \partial_z(s^2 z(1-z) \partial_z F) = 0.$$

Usually the line $a + b = 1$ intersects hyperbola $ab = (s-1)/s^2$ at two distinct points, while preserving reflection symmetry across the line $a = b$. Setting $s = 2$, the line $a + b = 1$ lays tangent to the hyperbola $ab = 1/4$ at the symmetry point $a = b = 1/2$, as in Fig. 2. The choice $s = 2$ also recovers the pendulum's characteristic differential equation, thus the appearance of integer 4 acquires a special meaning through the hypergeometric theory. The decomposition of 4 to $(a, b, c) = (1/2, 1/2, 1)$ produces all the necessary parameters to construct a series solution of the simple pendulum's period (Cf. Ref. [6], Ch. 5).

Euler and Gauss developed a fine characterization of the gross dynamics of a simple pendulum, but left exact solution of the time parameterization problem mostly an open question for the next few generations of researchers. The answering involved an honor roll of European patriarchs—Legendre, Riemann, Jacobi, Weierstrass and many others. Especially through the efforts of Abel (1802-1829), a central theme emerged that the time parameter can also take on complex values⁵. Subsequently during XX century the pendulum's exact solution in terms of standardized, doubly-periodic elliptic functions became a lauded final product of the classical era.

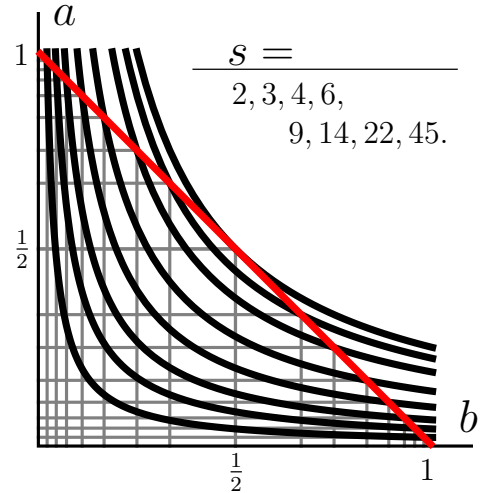


FIG. 2. Mapping between parameters.

The XX century also saw the advent of Quantum Mechanics. During this time period, precise spectroscopic measurement of atoms and molecules confounded preexisting theories; however, physicists did ultimately discover that classical oscillations have somewhat odd counterparts in the quantum regime. Initial attempts to describe quantum oscillations built upon the concept of phase space. The mathematical prehistory of phase space goes back to Poincaré (1854-1912), but the work of Ehrenfest (1880-1933) marks the first occurrence

⁵ For another closely related historical account, try *What is the Genus?*[7].

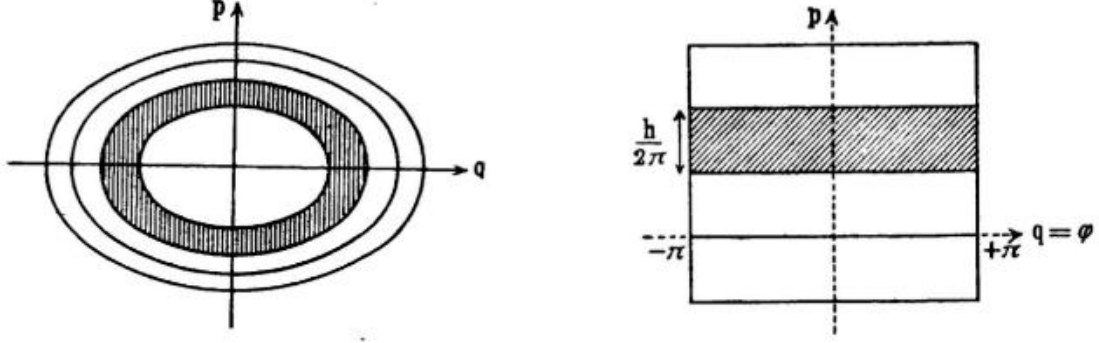


FIG. 3. Sommerfeld's phase plane geometries. (Source: Public Domain via archive.org)

of the the Deutsch word *Phasenraum*[8]. Thereafter Sommerfeld (1868-1951) included early depictions of two equivalent phase plane geometries in his famous text *Atombau Und Spektrallinien* [9]. To the uninitiate, the two drawings reproduced here in Fig. 3, are only curious works of abstract art. It is not immediately apparent that they describe harmonic oscillation, nor that they relate by a special coordinate transformation, nor that they can be deformed to account for non-linearity. These few basic facts of Hamiltonian Mechanics were widely understood by the last generation of classical analysts, and they are still important today⁶.

Modern texts follow and expound upon the figure drawing of Sommerfeld and others, making Hamiltonian mechanics an attractive and delightful subject, especially for visual learners and abstract free-thinkers. The pendulum phase portrait, here Fig. 4, is an iconic standard. Both popular and specialist accounts⁷ usually include such a figure when developing the visual language. The more demanding references typically ask the student not only to recreate the figure drawing, but also to measure its dimensions in terms of a period integral. Strangely enough, the standard solution does not usually involve much geometry, instead shows that a pendulum's dimensionless falling/rising velocity \dot{w} along the vertical coordinate w satisfies an algebraic constraint, $\dot{w}^2 = \frac{1}{4}w(1-w)(1-\alpha w)$. Change of variables by $w = \sin(\phi)^2$ then yields the textbook form,

$$T(\alpha) = 2 \int_0^1 \frac{dw}{\sqrt{w(1-w)(1-\alpha w)}} = \oint \frac{d\phi}{\sqrt{1-\alpha \sin(\phi)^2}}.$$

⁶ Especially in the development of *The Semiclassical Way*[10].

⁷ For example: [2] Chapter 11; [11] Chapter 6; [12] Unit 2, Chapter 7, etc.

Avoiding standards mimicry, we will use geometric methods to find, and to prove valid, a canonical Hamiltonian formulation where $q/p = \tan(\phi)$ and $\dot{\phi} = \sqrt{1 - \alpha \sin(\phi)^2}$. Discovery (or rediscovery) of the algebraic Hamiltonian function $2H(p, q) = (p^2 + q^2)(1 - \frac{1}{4}q^2)$ leads not only to quick derivation of the period integral, but also to an exact solution of the time parameterization problem via the Harold Edwards theory of elliptic curves and functions.

The article "A normal form for elliptic curves" testifies to Abel's inspirational genius, and stands as a paragon specimen of how mathematicians and scientists can use writing to promote alternative perspectives, fair attribution, and historical continuity [13]. History leads Edwards and his readers to a thoughtful and self-consistent revision of elliptic function theory. Simplification by symmetry is an important theme in this work of pure mathematics, but the results are not solely the product or possession of a leisure class. Interdisciplinary applications are part of the history and its followings. In cryptography, the simplified addition rule helps to optimize implementations of the widely-used Diffie-Hellman key-exchange protocol. Thus computer scientists have been among the first to accept and utilize the alternative paradigm. Edwards's normal form also presents physicists with an opportunity to break free from the confines of disciplinary boundaries and standard formulae⁸. Perhaps the future will have a better role for "Hamilton-Abel theory" than that of a clever joke or an idle dream. We will now commence an effort to synthesize physical Hamiltonian theory with the complex mathematics present in Harold Edwards's original masterpiece.

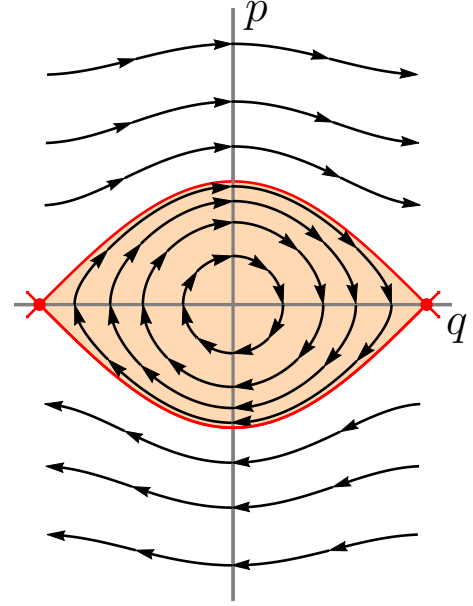


FIG. 4. Pendulum Phase Portrait.

⁸ As hinted during "ECCHacks" at Chaos Communication Congress 2014 [14].

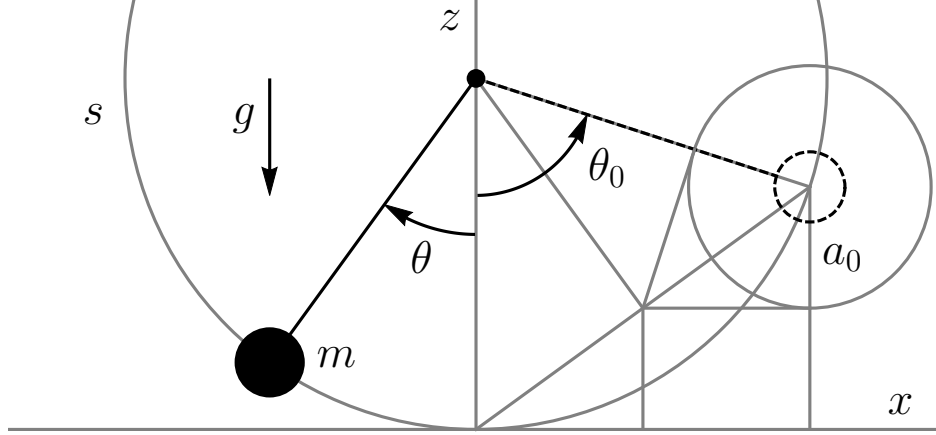


FIG. 5. Simple Pendulum Geometry.

II. PRELIMINARY ANALYSIS

The simple pendulum consists of a massive bob attached by a solid rod, assumed massless, to an axle as in Fig. 5. Gravity acts on the bob with vertical force mg , and the attachment applies a response force. The rod feels extensive and compressive stresses, but is assumed to respond with zero strain. As time elapses the bob swings and undergoes periodic motion along a circular trajectory of radius l . In *librational motion* the signs of angular coordinate θ and angular velocity $\dot{\theta}$ alternate while the pendulum reaches extremum deflection at regular intervals throughout the experiment. The time of one complete oscillation is called the *period* and denoted

by symbol T . In the absence of frictional damping a time series starting from time $t = 0$ at initial angle θ_0 would have that $\theta(t) = \theta_0$ whenever $t/T \in \mathbb{N}$. More realistically, one period T_n separates successive maxima θ_n and θ_{n+1} , with a non-zero frictional loss $\delta\theta_n = \theta_{n+1} - \theta_n > 0$. Only in the limit where $\delta\theta_n$ approaches zero, period $T_n = T_{n+1}$ becomes an exactly integrable observable. We shall work out the theory assuming that $\delta\theta_n = 0$ regardless of n , while

TABLE I. More Parameters.

Symbol	Dimension
l	$[L]$
a_0	$[L]$
g	$[L] [T]^{-2}$
m	$[M]$
(<u>Length</u> , <u>Mass</u> , <u>Time</u>)	

postponing worries about fidelity to a followup article on experiment and data analysis.

The simple design of Fig. 5 involves a few free parameters, collected in Table I. None of the initial parameters have dimension $[T]$ for time, but $[T]$ does occur as a factor in the dimensions of g . Without loss of generality, the $[L][M][T]$ dimensional system allows us to fix three scale degrees of freedom, i.e. to choose the base units of length, mass, and time. The obvious choice $l = m = 1$ scales dimensions $[L]$ and $[M]$. Another sensible choice, that $g = 1$, forces $l/g = 1$, so also sets the $[T]$ -scale. Intuition can easily guess period T proportional to fixed time $\sqrt{l/g} = 1$. Such a guess pays no regard to the dimensionless amplitude parameter,

$$\alpha = a_0/l = \frac{1}{2}(1 - \cos(\theta_0)) = \sin(\theta_0/2)^2.$$

Parameter α presents a difficulty to dimensional analysis by allowing that T is a function and not just a single number. For any integer n , the quantity $\sqrt{l/g} \alpha^n$ has time dimension, as does any quantity $T \in \sqrt{l/g} \mathbb{Q}[[\alpha]]$. An Ansatz for the period function,

$$T(\alpha) = \sqrt{\frac{l}{g}} \sum_{n \geq 0} c_n \alpha^n,$$

includes infinitely many undetermined coefficients $c_n \in \mathbb{Q}$. These coefficients are not constrained by dimensional analysis. The task of determining them calls for a stronger approach, one predicated upon a combination of physical principle and integral calculus.

Let the simple pendulum move in the xz plane along the arc of a unit circle. Choosing the center at $(x, z) = (0, 1)$ requires that $x^2 + (z - 1)^2 = 1$, and that $x \dot{x} = (1 - z) \dot{z}$. By these two equations, the bivariate expression for conservation of energy, $2(2\alpha - z) = \dot{x}^2 + \dot{z}^2$, reduces to a univariate form, $\dot{z}^2 = 2z(2\alpha - z)(2 - z)$. Re-scaled variable $w = z/(2\alpha)$ enables neat expression of the rising/falling velocity, but even greater simplicity follows from the choice of $w = \sin(\phi)^2$. The period integral then takes the form given in the introduction. Quarter-period integral

$$K(\alpha) = T(\alpha)/4 = \int_0^{\pi/2} \frac{d\phi}{\sqrt{1 - \alpha \sin(\phi)^2}},$$

is such a famous standard that it has a long-winded name, *the complete elliptic integral of the first kind* [15]. By formally verifying that $T(\alpha) = 4K(\alpha)$, part (a) of the typical textbook exercise is already completed. More challenging part (b) asks for a closed form for

the coefficients c_n . Term-by-term integration of the series expansion⁹ yields an exact solution in series,

$$T(\alpha) = \oint \frac{d\phi}{\sqrt{1 - \alpha \sin(\phi)^2}} = \sum_0^{2\pi} \frac{1}{4^n} \binom{2n}{n} \alpha^n \oint \sin(\phi)^{2n} = 2\pi \sum_0^{2\pi} \frac{1}{16^n} \binom{2n}{n}^2 \alpha^n.$$

If parts (a) and (b) are too easy, part (c) asks for proof that $c_n = \frac{2\pi}{16^n} \binom{2n}{n}^2$ satisfies $(n+1)^2 c_{n+1} = (n+1/2)^2 c_n$, and consequently that $K(\alpha)$ satisfies a particular hypergeometric differential equation¹⁰. Unfortunately the answers to parts (a), (b), and (c), do not contribute at all to intuition for the mysterious variable ϕ . They are not so much answers, but instead a distraction from deeper inquisition. Why does change of variables from z to ϕ work so well? Does simplicity indicate a hidden meaning for ϕ ? Is ϕ actually the angle of some particular geometric figure?

Recall that each libration cycle involves an alternating pattern of extrema,

$$\max(\dot{\theta}) \xrightarrow{K} \max(\theta) \xrightarrow{K} \min(\dot{\theta}) \xrightarrow{K} \min(\theta) \xrightarrow{K} \max(\dot{\theta}),$$

separated by equal time intervals of length $K(\alpha)$. This notation suggests that the abstraction ϕ relates somehow to the phase between hanging angle θ and its angular velocity $\dot{\theta}$. A simple hypothesis makes ϕ the angle of a polar coordinate system where $\theta = r \sin(\phi)$ and $\dot{\theta} = r \cos(\phi)$. If correct, the hypothesis should enable another derivation of the exact same integrand $d\phi/\dot{\phi}$. Gravitational force $mg = 1$ downward along the vertical results in a partial force along the tangent of motion, which affects an angular acceleration, and by Newton's laws, $\ddot{\theta} = -\sin(\theta)$. The phase angular velocity,

$$\begin{aligned} \dot{\phi} &= \cos(\phi)^2 \frac{d}{dt} \tan(\phi) = \frac{\dot{\theta}^2}{\theta^2 + \dot{\theta}^2} \frac{d}{dt} \left(\frac{\theta}{\dot{\theta}} \right) = \frac{\dot{\theta}^2 - \theta \ddot{\theta}}{\theta^2 + \dot{\theta}^2}, \\ &= \cos(\phi)^2 + \frac{\sin(\phi)}{r} \sin(r \sin(\phi)) = 1 + \sum_{n>0} \frac{(-1)^n}{(2n+1)!} r^{2n} \sin(\phi)^{2n+2}, \end{aligned}$$

looks hopelessly complicated. It is about to get even worse. Conservation of energy, $4\alpha = \dot{\theta}^2 + 4\sin(\theta/2)^2$, determines r as a function of $\sin(\phi)$ and α by reversion of the series,

$$4\alpha = r^2 + 2 \sum_{n>0} \frac{(-1)^n}{(2n+2)!} (r \sin(\phi))^{2n+2}.$$

⁹ Using that $(1 - 4\Phi)^{-1/2} = \sum \binom{2n}{n} \Phi^n$ and that $\oint (2\cos(\phi))^{2n} = \binom{2n}{n}$. Cf. OEIS [16], A000984.

¹⁰ We leave this as an exercise for the reader. Cf. OEIS [16], A002894.

Fortunately, the current argument depends only on the linear variation of $T(\alpha)$. The inverse series takes a form $r^2 = 4\alpha + \mathcal{O}(\alpha^2)$, and substitution to $\dot{\phi}$ partially solves $T(\alpha)$,

$$T(\alpha) = \oint \frac{d\phi}{\dot{\phi}} = \oint d\phi \left(1 + \frac{2}{3}\alpha \sin(\phi)^4 + \mathcal{O}(\alpha^2) \right).$$

Integral identity $\oint d\phi \sin(\phi)^4 = 3/8$ ensures the correct value $c_1 = 1/4$. More importantly, the expansion shows by contradiction that $\tan(\phi) \neq \theta/\dot{\theta}$ because the linear term of $T(\alpha)$ is an integral of $\sin(\phi)^4$ rather than $\sin(\phi)^2$. The false hypothesis is not entirely a loss. Similarity between alternative calculations of $T(\alpha)$ supports the idea that ϕ could be a phase angle. To find and prove the correct geometry, we will next give a short development of Hamiltonian mechanics, including a few basic facts from transformation theory.

III. PHASE PLANE GEOMETRY

The *phase plane* is a two-dimensional, Euclidean vector space spanned by Cartesian (p, q) variables. These variables measure the state of a test mass as it undergoes classical motion along one dimension. A choice of coordinates involves infinitely many hidden degrees of freedom, so it is usually not true that p stands for momentum and q for position. Hamiltonian mechanics reserves the letters p and q for those *canonical coordinates*, which are defined to satisfy Hamilton's equations of motion,

$$\frac{d}{dt}(p, q) = (\dot{p}, \dot{q}) = \left(-\frac{\partial H}{\partial q}, \frac{\partial H}{\partial p} \right).$$

Additional variables H and t stand for the Hamiltonian energy function and the special time parameter, respectively. Again, we will assume $2H(p, q) = \alpha$ with $\dot{\alpha} = 0$, thus the Hamiltonian H uniquely determines the conserved total energy at any state-point (q, p) . A three-dimensional visualization of function $H(q, p)$ superposes a surface,

$$\mathcal{H} = \{ (p, q, \alpha) \in \mathbb{R}^3 : \alpha = 2 H(p, q) \},$$

above the phase plane. Level sets of surface \mathcal{H} project to phase curves,

$$\mathcal{C}_\alpha = \{ (p, q) \in \mathbb{R}^2 : \alpha = 2 H(p, q), (\dot{p}, \dot{q}) \neq (0, 0) \}.$$

The tangent expansion of phase curve \mathcal{C}_α at energy α ,

$$d\alpha = 0 = \frac{\partial H}{\partial p} dp + \frac{\partial H}{\partial q} dq = \dot{q} dp - \dot{p} dq,$$

requires the existence of an *invariant differential*, $dt = dp/\dot{p} = dq/\dot{q}$, which solves the linear constraint equation. The integral $t = \int dt$ determines the time parameter t of \mathcal{C}_α and, by inversion, solutions $q(t)$ and $p(t)$ to the equations of motion. At critical points where $(\dot{p}, \dot{q}) = (0, 0)$, a tangent does not exist. Instead, the solution, $p(t) = p(0)$ and $q(t) = q(0)$, follows from the constant value theorem.

In a case-by-case exposition of Hamiltonian mechanics, harmonic oscillation usually shows within the first few examples. The Hamiltonian,

$$2H(p, q) = \kappa_p p^2 + \kappa_q q^2, \quad (\kappa_p > 0, \kappa_q > 0)$$

describes a paraboloid \mathcal{H} , and the phase curves \mathcal{C}_α are concentric ellipses when $\alpha > 0$. At the point $(p, q) = (0, 0)$, the system reaches a stable minimum with $\alpha = 0$, positive principal curvatures, κ_p and κ_q , and harmonic frequency $\omega = \sqrt{\kappa_p \kappa_q}$. Up to an initial condition ϕ_0 , trigonometric functions,

$$\begin{aligned} p(t) &= \sqrt{\alpha/\kappa_p} \cos(\omega t + \phi_0) \\ q(t) &= \sqrt{\alpha/\kappa_q} \sin(\omega t + \phi_0), \end{aligned}$$

solve Hamilton's equations, $(\dot{p}, \dot{q}) = (-\kappa_q q, \kappa_p p)$. A guess-and-check strategy works fine when the derivatives of sine and cosine are already known; however, repeating the solution in polar coordinates helps to develop better insight.

Choosing dimensions $\kappa_p = \kappa_q = \omega$ puts paraboloid \mathcal{H} into a most symmetrical, circular form, as in Fig. 6. In polar coordinates, $(p, q) = (r \cos(\phi), r \sin(\phi))$, the Hamiltonian $2H(r) = \omega r^2$ depends only the radial coordinate and leaves the phase angle unconstrained. Conservation of energy sets radius $r = \sqrt{\alpha/\omega}$. Again from $\tan(\phi) = q/p$ it follows that $\dot{\phi} = (p\dot{q} - \dot{p}q)/r^2 = \omega$ and that $\phi = \omega t + \phi_0$. This calculation verifies the time parameterization, but more importantly allows proof, $\partial_r H(r) \neq \omega$, that r and ϕ do not make a pair of canonical coordinates. Instead, the canonical choice is $\lambda = r^2/2$, and then Hamilton's equations work perfectly well,

$$\dot{\phi} = \partial_\lambda H(\lambda) = \omega \quad \text{and} \quad \dot{\lambda} = -\partial_\phi H(\lambda) = 0.$$

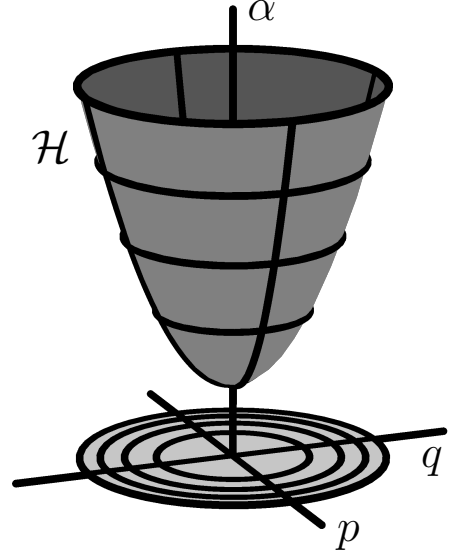


FIG. 6. A Circular Paraboloid \mathcal{H} .

This observation unlocks the secret of Sommerfeld's second drawing. It is a particularly plain picture of the harmonic oscillator phase curves in *action-angle* coordinates $(p, q) = (\lambda, \phi)$. Action-angle coordinates are an extremely useful tool, and worthy of a proper introduction.

When stated without blasé language, the changing of a phase ellipse into circular form gives a seminal example of canonical transformation theory. The squeeze transformation $(p_i, q_i) \rightarrow (p_f, q_f) = (p_i k, q_i/k)$ scales the phase plane by a dimensionless factor k . Choosing $k = (\kappa_p/\kappa_q)^{1/4}$ recovers $2H(q, p) = \omega(p^2 + q^2)$ from the earlier $2H(q, p) = \kappa_p p^2 + \kappa_q q^2$. Hamilton's equations remain invariant,

$$(\dot{p}_i, \dot{q}_i) = \left(-\frac{\partial H}{\partial q_i}, \frac{\partial H}{\partial p_i} \right) \longrightarrow (\dot{p}_f/k, \dot{q}_f k) = \left(-\frac{\partial H}{\partial q_f}/k, \frac{\partial H}{\partial p_f} k \right),$$

as the extra factors k cancel. Similarly, factors of k cancel after transforming the area two-form, $dp \wedge dq$. This is no coincidence. When coordinate q holds constant, the tangent geometry requires that $dp/d\alpha = (2\dot{q})^{-1}$, and similar for $dq/d\alpha$ with p constant. After applying Stokes's theorem, the time integrand obtains a profound form, $dt = 2\partial_\alpha \int_H dp \wedge dq$. We can now ask a fundamental question: which coordinate transformations leave dt invariant, or equivalently, which transformations leave Hamilton's equations invariant?

Under a general transformation $(p_i, q_i) \rightarrow (p_f, q_f)$ the area form,

$$dp_f \wedge dq_f = \left(\frac{\partial p_f}{\partial p_i} dp_i + \frac{\partial p_f}{\partial q_i} dq_i \right) \wedge \left(\frac{\partial q_f}{\partial p_i} dp_i + \frac{\partial q_f}{\partial q_i} dq_i \right) = \det(J) dp_i \wedge dq_i,$$

scales according to the Jacobian matrix and its determinant,

$$J = \begin{bmatrix} \frac{\partial p_f}{\partial p_i} & \frac{\partial p_f}{\partial q_i} \\ \frac{\partial q_f}{\partial p_i} & \frac{\partial q_f}{\partial q_i} \end{bmatrix} \quad \text{and} \quad \det(J) = \frac{\partial p_f}{\partial p_i} \frac{\partial q_f}{\partial q_i} - \frac{\partial p_f}{\partial q_i} \frac{\partial q_f}{\partial p_i}.$$

After characterizing the inverse transform $(p_f, q_f) \rightarrow (p_i, q_i)$ with an analogous matrix \tilde{J} , action on the tangent vectors,

$$(dp_f, dq_f) = J \cdot (dp_i, dq_i) \quad \text{and} \quad (dp_i, dq_i) = \tilde{J} \cdot (dp_f, dq_f).$$

ensures a product to identity, $\tilde{J}J = \mathbb{I}$. Hamilton's equations transform accordingly,

$$(\dot{p}_f, \dot{q}_f) = \left(-\frac{\partial H}{\partial q_f}, \frac{\partial H}{\partial p_f} \right) \longrightarrow J \cdot (\dot{p}_i, \dot{q}_i) = P \cdot \tilde{J} \cdot P \cdot \left(-\frac{\partial H}{\partial q_i}, \frac{\partial H}{\partial p_i} \right),$$

with permutation matrices P such that $P \cdot J^{-1} \cdot P = J / \det(J)$. When $\det(J) = 1$, the area form and Hamilton's equations remain invariant. The change of coordinates is then said to be a *canonical transformation*. For example, the pair of Jacobians,

$$J = \begin{bmatrix} p_i & q_i \\ -q_i/(p_i^2 + q_i^2) & p_i/(p_i^2 + q_i^2) \end{bmatrix} \quad \text{and} \quad \tilde{J} = \begin{bmatrix} \cos(q_f)/\sqrt{2p_f} & -\sqrt{2p_f} \sin(q_f) \\ \sin(q_f)/\sqrt{2p_f} & \sqrt{2p_f} \cos(q_f) \end{bmatrix},$$

satisfy $\det(J) = \det(\tilde{J}) = 1$, thus action-angle coordinates $(p_f, q_f) = (\lambda, \phi)$ are proven canonical relative to position-momentum coordinates $(p_i, q_i) = (p, q)$. This fact also follows quite obviously from the simple calculation, $d\lambda \wedge d\phi = r dr \wedge d\phi$, because the right hand side reproduces the well-known area form of a polar coordinate system.

Though Jacobian matrices simplify validation of coordinate transformations, their content excludes any mention of time, energy, or the Hamiltonian function. The integral identity,

$$t = \int_0^t dt' = 2\partial_\alpha \iint_H dp \wedge dq = 2\partial_\alpha S(\alpha, p, q),$$

tells more, that time t depends on the area $S(\alpha, p, q)$ beneath curve \mathcal{C}_α and between a valid initial and final condition, (p_0, q_0) and (p, q) respectively. The Hamiltonian flow,

$$\mathcal{F} = \{(p, q, t) \in \mathbb{R}^3 : t = 2\partial_\alpha S(\alpha, p, q)\},$$

equates time evolution with a solid geometry in phase-space-time (Deutsch: *phasenraumzeit*). For

harmonic oscillation, we can choose initial conditions such that $2S(\alpha, \lambda, \phi) = (\phi/\omega) \alpha$, and then the flow goes along a helicoid spiral over circular phase curves. In Fig. 7, both flows repeat after a vertical time-translation of $T = 2\pi/\omega$, because any closed curve \mathcal{C}_α bounds an entire area, $S(\alpha) = \pi r^2 = (\pi/\omega)\alpha$. Amplitude independence of period T characterizes harmonic oscillation. Usually amplitude dependence cannot be avoided, so the harmonic equations of motion are, at best, only valid and useful as an approximation in the infinitesimal limit. More generally, *anharmonic oscillation* along curve \mathcal{C}_α returns to initial condition (p_0, q_0) after a period $T(\alpha)$, which characteristically *must vary* with energy α .

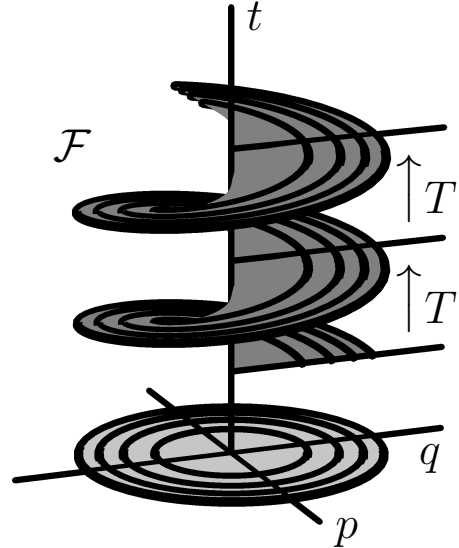


FIG. 7. A Helicoid Flow \mathcal{F} .

In the range of possible phase plane geometries, the most interesting cases involve a spatial admixture of qualitatively different critical points. In local coordinates (p, q) around a critical point at $(p, q) = (0, 0)$, assume the Hamiltonian becomes approximately quadratic, $2H \approx \kappa_p p^2 + \kappa_q q^2$. Then the sign of $\kappa_p \kappa_q$ distinguishes between circular points with $\kappa_p \kappa_q > 0$ and hyperbolic points with $\kappa_p \kappa_q < 0$. We have already seen that circular points imply local harmonic oscillation, but have yet to encounter hyperbolic points or the separatrix curves they pair with. Choosing coordinates where $2H = p^2 - q^2$, Hamilton's equations, $(\dot{p}, \dot{q}) = (q, p)$, are solved by hyperbolic trigonometric functions, $p(t) = \sqrt{\alpha} \cosh(t)$ and $q(t) = \sqrt{\alpha} \sinh(t)$. Proof does not differ significantly from the earlier case of Harmonic oscillation. In fact, this similarity is the first sign of an even deeper transformation theory, which we will eventually take up and explore in detail.

Around a hyperbolic point, the Hamiltonian factors, $2H = (p+q)(p-q)$. Lines determined by $p+q = 0$ and $p-q = 0$ intersect at the hyperbolic point. A separatrix curve, with $\alpha = 0$, extends from those two lines outwards to the wider area of the phase plane. When the Hamiltonian contains terms higher than quadratic, a line leaving the hyperbolic point can possibly change direction. Then the separatrix segment either goes off to infinity, or it may return along another direction to the initial hyperbolic point, or it may even approach a second, distinct hyperbolic point. Taking a union over disjoint segments, the *separatrix* curve is so named because, globally, it separates phase space into qualitatively different, non-intersecting subsets. For example, the red separatrix curve of Fig. 4 separates the phase portrait into regions where the pendulum rotates either clockwise or counterclockwise, and another central region where libration occurs.

A general *oscillation disk* in the phase plane is defined as a topological disk bounded by a separatrix at energy α_1 , which additionally contains exactly one critical point, a circular point at energy α_0 . This domain also contains anharmonic oscillation within the energy range $\alpha \in (\alpha_0, \alpha_1)$. Level curves around the circular point gradually deform away from a circular shape, but must retain loop topology. When a curve accumulates non-constant variation of curvature, the phase angular velocity $\dot{\phi}$ measures change of shape, as in Fig. 8. Most obviously, the heatmaps show slowing around the hyperbolic points, where the limit $\alpha \rightarrow \alpha_1$ causes an interval of the curve \mathcal{C}_α to pinch into a corner. These extreme deformations force $\dot{\phi}$ to approach zero locally, and the integral period function diverges.

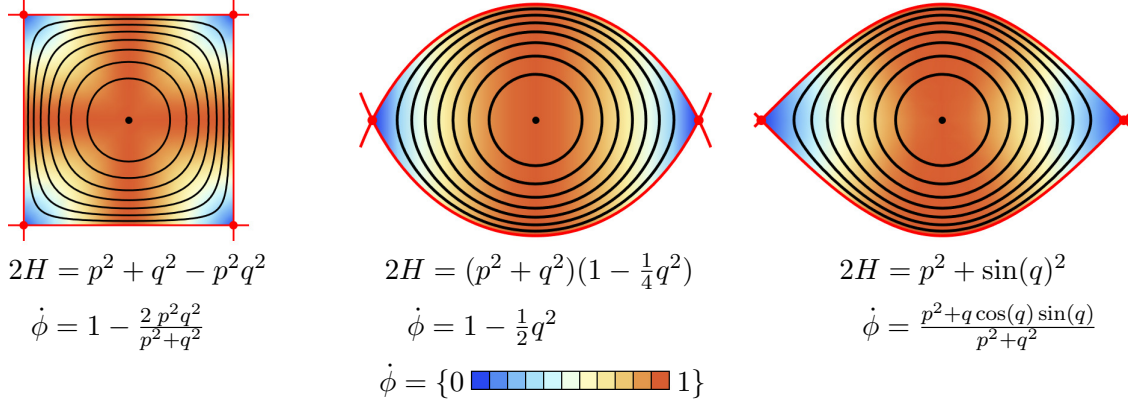


FIG. 8. A Few Oscillation Disk Heatmaps, Colored by $\dot{\phi}$.

Choosing canonical coordinates $(p, q) = (\dot{\theta}, \theta)/2$, the Hamiltonian function,

$$\alpha = 2H(p, q) = p^2 + \sin(q)^2,$$

models the motion of a simple pendulum. In the energy range $0 < \alpha < 1$, the curve geometry unifies to an oscillation disk, as in the left of Fig. 8. The tangent expansion fails not only at the circular point $(q, p) = (0, 0)$, but also at the hyperbolic points $(p, q) = (0, \pm\pi/2)$. The period function must increase from its harmonic limit at $\alpha = 0$ to an infinite divergence at $\alpha = 1$. Limiting analysis recapitulates what we should already know from preliminary analysis and laboratory experiments. At small amplitudes, the pendulum oscillates harmonically around the stable minimum. Larger amplitude oscillations eventually reach an inverted configuration where the force of gravity has only a small component along the direction of motion. Thus slowing occurs on approach to the unstable equilibrium point.

The mere existence of singular divergences suggests that ordinary differential equations could be a useful tool for rigorously defining the pendulum's period function. At first we will prefer an easier, more direct analysis. Up to a second power of the action variable λ , the pendulum's Hamiltonian may be approximated as $\alpha/2 = H(\lambda, \phi) = \lambda - \frac{2}{3}\lambda^2 \sin(\phi)^4$. Quadratic root solving yields twice the action $2\lambda = \frac{3}{2} \frac{1}{\sin(\phi)^4} \left(1 - \sqrt{1 - \frac{4}{3}\alpha \sin(\phi)^4}\right)$, and by the chain rule,

$$T(\alpha) = \oint \frac{d\phi}{\dot{\phi}} = 2 \oint d\phi \partial_\alpha \lambda = \oint \frac{d\phi}{\sqrt{1 - \frac{4}{3}\alpha \sin(\phi)^4}} = 2\pi \left(1 + \frac{1}{4}\alpha + \frac{35}{192}\alpha^2 + \dots\right).$$

This is a nice and easy trick! It gets the linear term correct, without any need for series reversion. However, the sine function is bounded by ± 1 , so the denominator goes to zero

when $\alpha = 3/4$, and the critical points fall short at $|q| = \sqrt{3/2} < \pi/2$. After c_0 and c_1 , all coefficients c_n with $n > 1$ are overestimates¹¹. Instead, let us introduce an arbitrary trigonometric polynomial Φ and replace $(4/3)\sin(\phi)^4 \rightarrow \Phi$. When $\Phi = \sin(\phi)^2$, the root solving procedure reproduces the correct period function.

As Φ multiplies λ^2 in the Hamiltonian, any valid perturbing term needs Φ to be a homogeneous quartic polynomial in the variables $P = \cos(\phi)$, $Q = \sin(\phi)$. The quadratic choice $\Phi = Q^2$ obviously does not satisfy the validity constraint, but a workaround is available via the Pythagorean theorem, $P^2 + Q^2 = 1$. Multiplication of Φ by the algebraic unit $P^2 + Q^2$ raises the polynomial degree by +2. This allows a quartic choice $\Phi = (Q^2 + P^2)Q^2$, which may reduce to $\Phi = Q^2$, but also identifies with a valid perturbing term. The algebraic Hamiltonian $2H(q, p) = (q^2 + p^2)(1 - \frac{1}{4}q^2)$ transforms canonically to its action-angle form, $H(\lambda, \phi) = \lambda - \frac{1}{2}\lambda^2 \sin(\phi)^2$, again quadratic in the variable λ . This geometry includes an oscillation disk in the energy range $0 < \alpha < 1$, which appears in the center of Fig. 8. By design, the quarter period of H is $K(\alpha)$.

Determination of isoperiodicity suggests that the two Hamiltonian models,

$$2H_i(q, p) = p^2 + \sin(q)^2 \quad \text{and} \quad 2H_f(q, p) = (p^2 + q^2) \left(1 - \frac{1}{4}q^2\right),$$

will equate, $H_i(q_i, p_i) = H_f(q_f, p_f)$, by a canonical transformation between initial and final coordinates. A plausible guess that $p_i \dot{q}_i = p_f \dot{q}_f$ gives a second constraint equation in two unknowns. The non-linear system can be solved for either,

$$\begin{aligned} (p_i, q_i) &= \left(\frac{1}{2} p_f \sqrt{4 - q_f^2}, \arcsin \left(\frac{1}{2} q_f \sqrt{4 - q_f^2} \right) \right) \quad \text{or} \\ (p_f, q_f) &= \pm \left(\csc(q_i) p_i \sqrt{2 - 2 \cos(q_i)}, \sqrt{2 - 2 \cos(q_i)} \right), \end{aligned}$$

and the Jacobian matrices are written out as,

$$J = \pm \begin{bmatrix} \sqrt{2 - 2 \cos(q_i)} \csc(q_i) & \frac{p_i \tan(q_i/2)^2}{\sqrt{2 - 2 \cos(q_i)}} \\ 0 & \frac{\sin(q_i)}{\sqrt{2 - 2 \cos(q_i)}} \end{bmatrix} \quad \text{and} \quad \tilde{J} = \begin{bmatrix} \frac{\sqrt{4 - q_f^2}}{2} & -\frac{p_f q_f}{2\sqrt{4 - q_f^2}} \\ 0 & \frac{2}{\sqrt{4 - q_f^2}} \end{bmatrix},$$

while requiring that $|q_f| \leq \sqrt{2}$. The domain restriction is permissive enough to map between entire oscillation disks. According to the determinants, $\det(J) = \det(\tilde{J}) = 1$, the

¹¹ It should be possible to prove this assertion by induction on n .

transformation is verified canonical. This calculation shows that ϕ is indeed a canonical coordinate of the pendulum Hamiltonian. Solution of $\theta(t)$ follows from any solution of $\lambda(t)$ and $\phi(t)$, one of which we will now pursue in even more detail.

IV. INCORPORATING COMPLEX TIME

Harold Edwards's theory of elliptic curves and elliptic functions starts with an alternative normal form, $x^2 + y^2 = a^2 + a^2 x^2 y^2$. The crucial elliptic function,

$$\psi(t) = \chi(t + \tfrac{1}{2}) = \frac{2 \sum_{n=1}^{\infty} e^{i\pi(2n-1)^2 \tau/2} \cos((2n-1)\pi t)}{1 + 2 \sum_{n=1}^{\infty} e^{i\pi(2n)^2 \tau/2} \cos(2n\pi t)},$$

allows a solution, $x(t) = \chi(t)$ and $y(t) = \psi(t)$, of the coupled differential equations¹², $\dot{x} = y(1 - a^2 x^2)$ and $\dot{y} = -x(1 - a^2 y^2)$, and the solution must adhere to the normal form. Edwards already proves this statement in Part III of the original article [13]. Translation of his solution to the simple pendulum context encounters two difficulties. First, a transformation is needed to go from math coordinates (x, y) to physical coordinates (p, q) —but this follows quickly from the previous developments. Second, and with more effort, calculation of the correct value for the period ratio τ depends upon ascertainment of the double-periodicity notion. To this end, the Wick rotation, $t \rightarrow it$, helps to extend transformation theory, and to show relation between real and complex periods.

Let us introduce a function G such that $2G = (x^2 + y^2) - a^2 x^2 y^2 - a^2$, and utilize G to determine a family of elliptic curves, $\mathcal{C}_a = \{(x, y) : 2G(x, y, a) = 0\}$. In a sense, function G is Hamiltonian with canonical coordinates x and y ; however, the analogy can be improved. Transforming coordinates by $(G, a, x, y) \rightarrow (H, \alpha, p, q) = (a^2 G, a^4, a y, a x)$ produces a Hamiltonian form, $\alpha = 2H = p^2 + q^2 - p^2 q^2$. In action angle coordinates, the Hamiltonian becomes $H = \lambda - \frac{1}{2} \lambda^2 \sin(2\phi)^2$. Anharmonic oscillation occurs with real period,

$$T(\alpha) = 4K(\alpha) = \oint \frac{d\phi}{\sqrt{1 - \alpha \sin(2\phi)^2}},$$

and an exact parameterization $p(t) = \alpha^{1/4} \psi(t)$, $q(t) = \alpha^{1/4} \chi(t)$. Another transformation, $(t_i, \phi_i) \rightarrow (t_f, \phi_f) = 2(t_i, \phi_i)$, is not canonical, but nevertheless preserves Hamilton's

¹² Edwards's normalization of the time domain requires chain rule, $\dot{\psi} = (2/T)d\psi/dt$, with real period T .

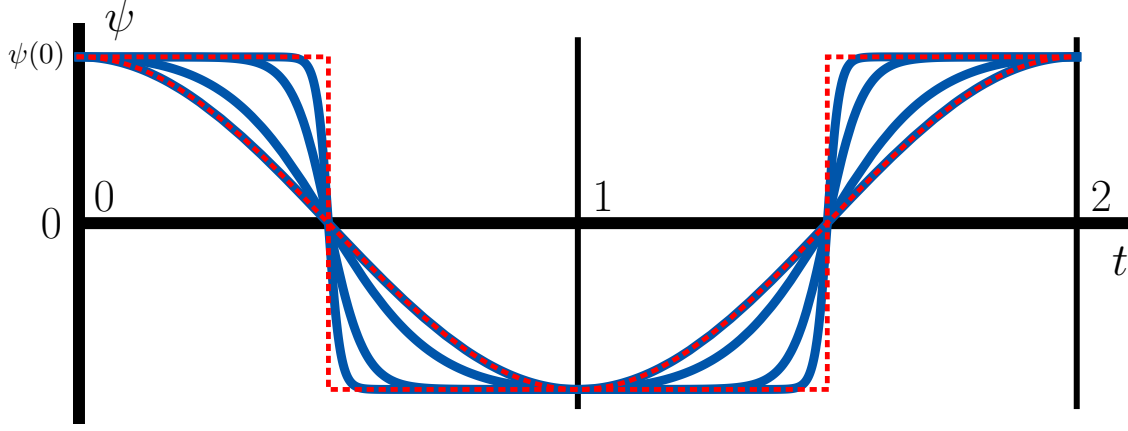


FIG. 9. Real-Valued Slices of the Elliptic Function $\psi(t)$; $\Im(t) = 0$ and $\tau = \{i, \frac{i}{3}, \frac{i}{9}, \frac{i}{27}\}$.

equations covariantly¹³. Angle doubling allows exact solution,

$$\lambda(t) = \frac{\sqrt{\alpha}}{2} \left(\chi\left(\frac{t}{2}\right)^2 + \psi\left(\frac{t}{2}\right)^2 \right), \quad \phi(t) = \arctan \left(\chi\left(\frac{t}{2}\right) / \psi\left(\frac{t}{2}\right) \right),$$

of the earlier pendulum model, $H = \lambda - \frac{1}{2}\lambda^2 \sin(\phi)^2$. Time parameterization for pendulum variables θ and $\dot{\theta}$ then follows by walking back (λ, ϕ) through the sequence of canonical transformations—first to the cartesian coordinates,

$$p(t) = \frac{\psi\left(\frac{t}{2}\right)^2 - \chi\left(\frac{t}{2}\right)^2}{\left(1 + \chi\left(\frac{t}{2}\right)^2 \psi\left(\frac{t}{2}\right)^2\right)^{\frac{1}{2}}}, \quad q(t) = \frac{2 \chi\left(\frac{t}{2}\right) \psi\left(\frac{t}{2}\right)}{\left(1 + \chi\left(\frac{t}{2}\right)^2 \psi\left(\frac{t}{2}\right)^2\right)^{\frac{1}{2}}},$$

of $2H = (p^2 + q^2)(1 - \frac{1}{4}q^2)$, then to the pendulum coordinates,

$$\theta(t) = 2 \arcsin \left(\frac{2 \chi\left(\frac{t}{2}\right) \psi\left(\frac{t}{2}\right)}{1 + \chi\left(\frac{t}{2}\right)^2 \psi\left(\frac{t}{2}\right)^2} \right), \quad \dot{\theta}(t) = 2 \left(\frac{\psi\left(\frac{t}{2}\right)^2 - \chi\left(\frac{t}{2}\right)^2}{1 + \chi\left(\frac{t}{2}\right)^2 \psi\left(\frac{t}{2}\right)^2} \right).$$

The expression for $\theta(t)$ reduces again according to a special case of the X addition rule, proven in Part II of [13]. The addition rules act linearly along the time dimension, so the choice of $x' = x = \chi(\frac{t}{2})$ and $y' = y = \psi(\frac{t}{2})$ sets $X = \chi(t)$, and also,

$$\theta(t) = 2 \arcsin \left(\alpha^{1/4} \chi(t) \right).$$

Yet this formal solution is worthless until we have defined the period ratio τ as a function of the energy parameter α . In context, the correct answer is that $\tau = i \frac{K(1-\alpha)}{2K(\alpha)}$, but again, why?

¹³ Covariant: $|J| = \frac{\partial t_f}{\partial t_i}$. Two non-canonical transformations act together as a canonical transformation.

The real period $T(\alpha)$ itself gives a first hint of double-periodicity, because it satisfies a second order differential equation. A proof of the assertion depends upon an annihilator \mathcal{A} and its certificate function Ξ ,

$$\mathcal{A} = 1 - 4(1 - 2\alpha)\partial_\alpha - 4\alpha(1 - \alpha)\partial_\alpha^2 \quad \text{and} \quad \Xi_n = \frac{\sin(2n\phi)}{2n(1 - \alpha\sin(n\phi)^2)^{3/2}}.$$

The zero sum,

$$\mathcal{A} \circ \left(\frac{1}{\sqrt{1 - \alpha\sin(n\phi)^2}} \right) - \partial_\phi \Xi_n = 0,$$

is trivial to verify by applying chain rule and reducing trigonometric terms. Integration of any exact differential along a complete cycle yields a zero, including $\oint d\phi \partial_\phi \Xi_n = 0$, thus the claim, $\mathcal{A} \circ T(\alpha) = 0$, stands true. The transformation $\alpha \rightarrow 1 - \alpha$ leaves \mathcal{A} invariant, so the general solution of the second order differential equation can be written as $T(\alpha) = c_1 K(\alpha) + c_2 K(1 - \alpha)$. This solution space includes two special solutions, the real and complex periods, $T_{\Re}(\alpha) = 4K(\alpha)$ and $T_{\Im}(\alpha) = i2K(1 - \alpha)$, whose ratio reproduces the suggested form $\tau = T_{\Im}(\alpha)/T_{\Re}(\alpha)$. The hint seems to have paid off, but leaves room for doubt and suspicion.

We do not yet have a physical reason to complexify the time variable by extending from a one-dimensional real axis to a two-dimensional complex plane; however, mathematical function theory calls ahead of schedule for just such an abstraction. To account for additional complex degrees of freedom, we will build out a Riemann surface¹⁴,

$$\mathcal{R}_\alpha = \{(p, q) \in \mathbb{C}^2 : \alpha = 2H(p, q)\} \simeq \{(v, w, x, y) \in \mathbb{R}^4 : \alpha = 2H(x + iv, y + iw)\},$$

around each phase curve \mathcal{C}_α . If transformation of canonical p and q variables introduces determinant $|J| \in \mathbb{C}/\{0, 1\}$, then neither the two-form $dp \wedge dq$, nor the time scale dt , nor Hamilton's equations will preserve. However, it is possible to cancel the extra factor $|J|$ by scaling time covariantly, $t_i \rightarrow t_f = |J| t_i$. Any transformation with unit modulus $|J|$ acts as rotation on the complex t -plane. In particular, the Wick rotation, $t_i \rightarrow t_f = i t_i$, goes by $\pi/2$ radians through the time plane, thus permutes real and complex axes. The simplest covariant coordinate transformation having $|J| = i$ takes $p_i \rightarrow p_f = i p_i$ and rotates \mathcal{R}_α by

¹⁴ The nomenclature "Kleinian Surface" may be better. Jeremy Gray claims that Felix Klein was the first to think of an algebraic curve as "a closed surface in its own right" [17].

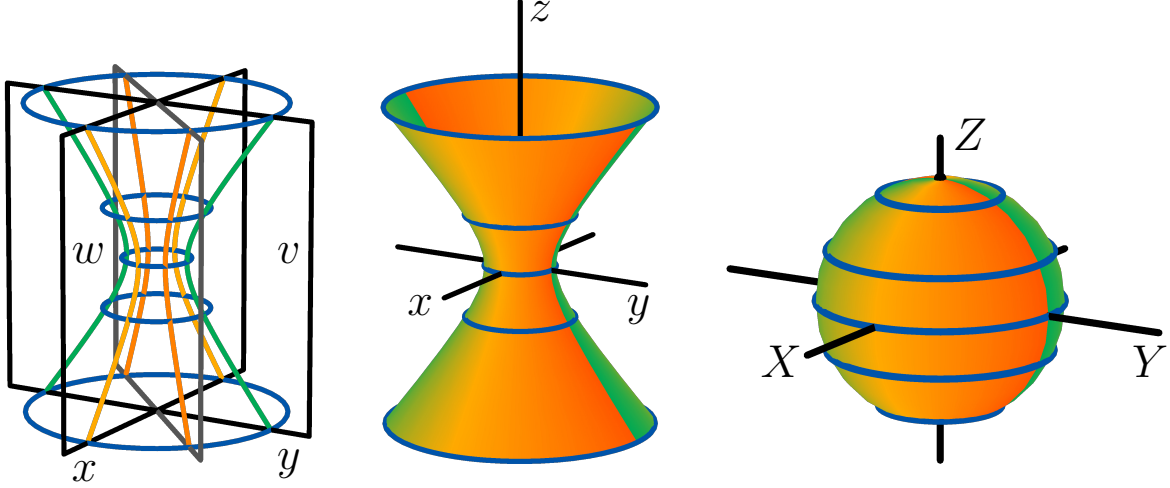


FIG. 10. A Few Depictions of a Genus Zero Riemann Surface.

$\pi/2$ radians through a four dimensional space $\mathbb{C}^2 \simeq \mathbb{R}^4$. Covariant Wick rotation is another neat trick, which ultimately allows calculation of the complex period on doubly-periodic \mathcal{R}_α by integration along a real-valued level curve $\tilde{\mathcal{C}}_\alpha$. Before moving ahead to non-trivial topology, it is worthwhile to work through the simplest example in genus zero.

Real-valued theory distinguishes between circular points and hyperbolic points, while complex-valued theory does not. Any transformation such as $(p_i, q_i) \rightarrow (p_f, q_f) = (i p_i, q_i)$ changes constraints, from circular $\alpha = 2H = p^2 + q^2$ to hyperbolic $\alpha = 2\tilde{H} = -p^2 + q^2$, and *vice versa*. It is possible to embed the entire *harmonic hyperboloid* into three dimensions,

$$\mathcal{R}_\alpha = \{(p, q) \in \mathbb{C}^2 : \alpha = p^2 + q^2\} \rightarrow \mathcal{S}_\alpha = \{(x, y, z) \in \mathbb{R}^3 : \alpha + z^2 = x^2 + y^2\},$$

while loosing only a phase degree of freedom via the map $(v, w) \rightarrow z = \pm\sqrt{v^2 + w^2}$. More explicitly, \mathcal{S}_α is obtained from \mathcal{R}_α after considering rotational symmetry in the (p, q) -plane. Coordinates $x = w = 0$ and $z = v$ may be chosen such that $\tilde{\mathcal{C}}_\alpha = \{(y, z) : \alpha = -z^2 + y^2\}$ is a hyperbola connected to the base circle $\mathcal{C}_\alpha = \{(x, y) : \alpha = x^2 + y^2\}$ at the turning points $(p, q) = (0, \pm\sqrt{\alpha})$. Any other point $(p, q) = (x_0, y_0)$ along \mathcal{C}_α is yet again a turning point; however, in a rotated coordinate system. Point (x_0, y_0) connects circular \mathcal{C}_α to a *rotated copy* of hyperbolic $\tilde{\mathcal{C}}_\alpha$, which falls in the hyperplane determined by $(x_0 u + y_0 v)(x_0 y - y_0 x) = 0$.

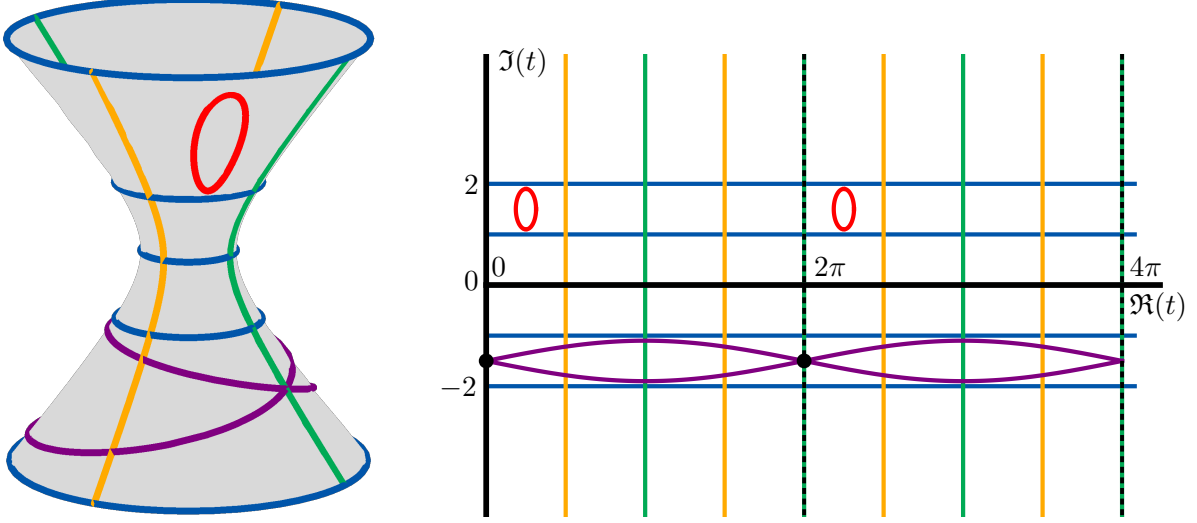


FIG. 11. Genus Zero Harmonic Hyperboloid and Singly-Periodic Uniformization.

Two equivalent parameterizations,

$$\mathcal{R}_\alpha = \left\{ (p, q) = \left(\sqrt{\alpha} \sin(t), \sqrt{\alpha} \cos(t) \right) \in \mathbb{C}^2 : t \in \mathbb{C} \right\},$$

and

$$\tilde{\mathcal{R}}_\alpha = \left\{ (p, q) = \left(\sqrt{\alpha} \sinh(u), \sqrt{\alpha} \cosh(u) \right) \in \mathbb{C}^2 : u \in \mathbb{C} \right\},$$

of the harmonic hyperboloid follow from the solution of Hamilton's equations, around a circular point and a hyperbolic point respectively. Wick rotation $t \rightarrow u = i t$ equates \mathcal{R}_α and $\tilde{\mathcal{R}}_\alpha$ up to a $\pi/2$ -radian rotation through the complex p -plane. While the usual trigonometric functions are periodic, their hyperbolic counterparts certainly are not. Taken together periodicity along $\Re(t)$ and non-periodicity along $\Re(u)$ implies genus zero. This identification introduces some cognitive dissonance, because the sphere is usually given as the standard form of a genus zero surface. In three dimensions, the hyperboloid,

$$\mathcal{S}_\alpha = \left\{ (x, y, z) = \left(\sqrt{\alpha} \sin(t) \cosh(u), \sqrt{\alpha} \cos(t) \cosh(u), \sqrt{\alpha} \sinh(u) \right) \in \mathbb{R}^3 : (t, u) \in \mathbb{R}^2 \right\},$$

transforms into the Riemann sphere by stereographic projection,

$$(x, y, z) \rightarrow (X, Y, Z) = \left(\frac{2\sqrt{\alpha} x}{\alpha + x^2 + y^2}, \frac{2\sqrt{\alpha} y}{\alpha + x^2 + y^2}, \pm \frac{(\alpha - x^2 - y^2)}{(\alpha + x^2 + y^2)} \right),$$

with $+$ chosen for $z \geq 0$ and $-$ chosen otherwise.

With two periods rather than just one, a genus one elliptic curve differs qualitatively from the genus zero harmonic hyperboloid. In general, the two periods may describe the

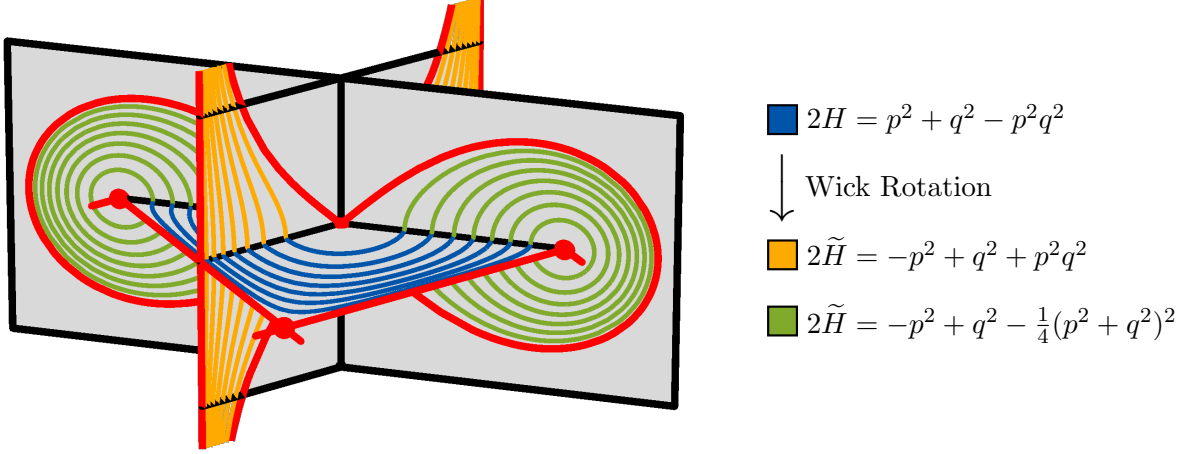


FIG. 12. Toric Cross Sections via Wick Rotation.

boundaries of a *period parallelogram* in the complex t -plane; however, in Edwards's normal form, a choice of real $\alpha \in (0, 1)$ amounts to choosing a *period rectangle* with entirely complex τ and $\Im(\tau) \in (0, \infty)$. To calculate τ explicitly, we transform by a Wick rotation, $H \rightarrow \tilde{H}$, as in Fig. 12. Both transforms introduce a factor $|J| = i$ relative to the initial choice of coordinates¹⁵. Constraint $\alpha = 2\tilde{H}$, for either \tilde{H} , cuts out a real-valued curve $\tilde{\mathcal{C}}_\alpha$. Hamilton's equations determine the complex period, up to a missing factor i . One choice leads to an easier integral,

$$T_{\mathfrak{J}}(\alpha) = i \oint dt = i \int_{-\infty}^{\infty} \frac{dp}{\sqrt{(1+p^2)(\alpha+p^2)}},$$

on a non-compact contour, while the other offers compactness with a harmonic limit $\omega = 2$ as $\alpha \rightarrow 1$. Integral value $T_{\mathfrak{J}}(1) = i\pi$ also implies that $\omega = 2\pi i/T_{\mathfrak{J}}(1) = 2$. More importantly, the zero sum,

$$\mathcal{A} \circ \frac{1}{\sqrt{(1+p^2)(\alpha+p^2)}} + \partial_p \tilde{\Xi} = 0, \quad \text{with} \quad \tilde{\Xi} = \frac{p(1+p^2)^{1/2}}{(\alpha+p^2)^{3/2}},$$

certifies that $\mathcal{A} \circ T_{\mathfrak{J}}(\alpha) = 0$, because $\int_{-\infty}^{\infty} dp \partial_p \tilde{\Xi} = 0$. The harmonic limit determines the constants of integration, and $T_{\mathfrak{J}}(\alpha) = i2K(1-\alpha)$, as desired. Depending on the reader's naiveté, it is either astounding or mundane that both real and complex solutions should satisfy the same differential equation. The cohomological theory of algebraic varieties gives

¹⁵ Easy Exercise: Prove $|J| = i$ explicitly, then prove the two alternatives canonically equivalent.

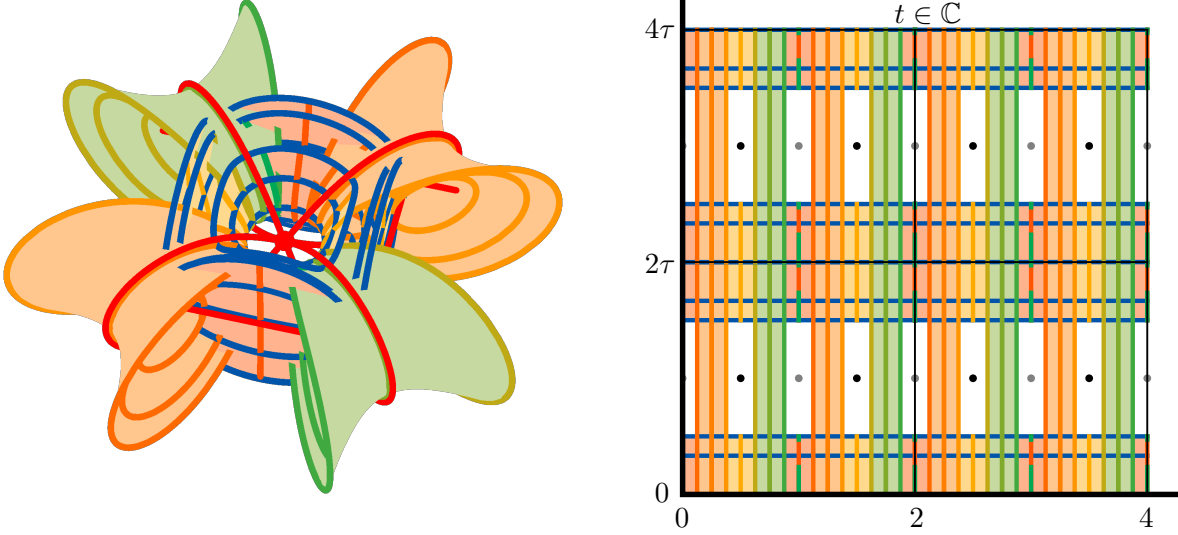


FIG. 13. Genus One Elliptic Curves and Doubly-Periodic Uniformization.

a standard mathematical explanation as to *why*, but for now we are more concerned with the ever-pressing *what for*.

Unlike their trigonometric counterparts, the shape of $\chi(t)$ or $\psi(t)$ depends on the amplitude parameter α via the period ratio $\tau = i \frac{K(1-\alpha)}{2K(\alpha)}$, now justly derived. Shape variation with α carries over to the Riemann surface,

$$\mathcal{R}_\alpha = \left\{ (p, q) = (\alpha^{\frac{1}{4}} \psi(t), \alpha^{\frac{1}{4}} \chi(t)) \in \mathbb{C}^2 : t \in \mathbb{C} \right\},$$

which limits to a central harmonic hyperboloid when $\alpha \rightarrow 0$ and $\Im(t) \rightarrow 2n i \tau$, $n \in \mathbb{Z}$. Around $\Im(t) = 0$, surface \mathcal{R}_α looks sufficiently like the harmonic hyperboloid to allow a similar embedding¹⁶,

$$\mathcal{S}_\alpha = \left\{ (x, y, z) = (\alpha^{\frac{1}{4}} \psi_{\Re}(t), \alpha^{\frac{1}{4}} \chi_{\Re}(t), \pm \alpha^{\frac{1}{4}} \sqrt{\chi_{\Im}(t)^2 + \psi_{\Im}(t)^2}) \in \mathbb{R}^3 : t \in \mathbb{R} \times [0, \pm \frac{\tau}{2}] \right\}.$$

Subscripts \Re and \Im indicate either the real or the imaginary component of complex-valued functions $\psi(t)$ and $\chi(t)$. Hyperbolic sections also expand over thin strip domains of width $\Delta t = 1/4$, centered on vertical lines $\Re(t) = (2n + 1)/4$, $n \in \mathbb{Z}$. Four sections in the range \mathbb{C}^2 separately approach a harmonic hyperboloid in the limit $\alpha \rightarrow 1$. In the right panel of Fig. 13, the partial domain of all five hyperbolic sections covers a full three-quarters of \mathbb{C} while avoiding points $\tau + n/2$, $n \in \mathbb{Z}$. At these points, either χ or ψ has a pole. Projecting

¹⁶ The map $(p, q) \rightarrow (x, y, z)$, from \mathcal{R}_α to \mathcal{S}_α , preserves the euclidean metric: $p^*p + q^*q = x^2 + y^2 + z^2$.

the disjoint pieces of \mathcal{R}_α to three dimensions and coloring by the real component of time, we expand from the skeleton of Fig. 12 to the patchwork surfaces nested in the left of Fig. 13. Admittedly, the result looks sketchy, but so far we have yet to do any better.

Depiction of complex tori flexes impressive strength, but actually requires considerably more effort than is necessary for applications in physics. With only values of $\psi(t)$ above the real time axis, we can graph sections of a Hamiltonian flow and make a wide range of experimental predictions—the two tasks are not really any different. Fig. 14 depicts a section of the pendulum’s Hamiltonian flow,

$$\mathcal{F}_\alpha = \left\{ \left(\frac{1}{2}\theta(t), \frac{1}{2}\dot{\theta}(t), 2K(\alpha)t \right) \in \mathbb{R}^3 : t \in \mathbb{R} \right\},$$

along with equivalent flows conformed to the algebraic models. In terms of textbook expectations, these graphs leave little to be desired, save a few numerical double-checks. The following zero sums,

$$0 = 2H(q(t), q(t)) - \alpha, \quad 0 = \dot{p}(t) + \partial_q H|_t, \quad 0 = \dot{q}(t) - \partial_p H|_t,$$

can be evaluated for real sample points $t \in [0, 2]$ and $\alpha \in (0, 0.99)$. A truncation of ψ after five summation terms is sufficient to converge to machine precision, $0 \approx 10^{-15}$. This agreement should dispel any remaining doubt about veracity of the solution, but if necessary, testing can be extended to higher values $\alpha \in (.99, 1)$ and to arbitrary precision simply by including more summation terms.

Even then, those more inclined to standard methodology can be expected to issue an obstinate argument that "Hamilton’s equations have a unique solution. For the simple pendulum, that solution is written in terms of the Jacobian Elliptic functions". Certainly this is also true [18, 19], and by comparison of *equally valid* solutions, we find that,

$$\operatorname{sn}(2K(\alpha)t|\alpha) = \alpha^{-\frac{1}{4}}\chi(t), \quad \operatorname{cn}(2K(\alpha)t|\alpha) = \frac{\psi(\frac{t}{2})^2 - \chi(\frac{t}{2})^2}{\chi(\frac{t}{2})^2 + \psi(\frac{t}{2})^2},$$

only where $\alpha \in (0, 1)$ and $\tau = i\frac{K(1-\alpha)}{2K(\alpha)} \in (0, \infty)$. These identities imply that any equations solvable in terms of the Jacobian elliptic functions are also solvable in terms of $\psi(t)$ with entirely imaginary τ . Allowing that $\tau \in \mathbb{C}$, the function $\psi(t)$ becomes fully as powerful as Weierstrass’s $\wp(t)$, i.e. it is the most general elliptic function possible. More work remains to be done. Wherever a standard solutions exists and is known, another alternative solution in terms of $\psi(t)$ is waiting to be found. What we have seen so far encourages the hope that new derivations will lead to even more new insight!

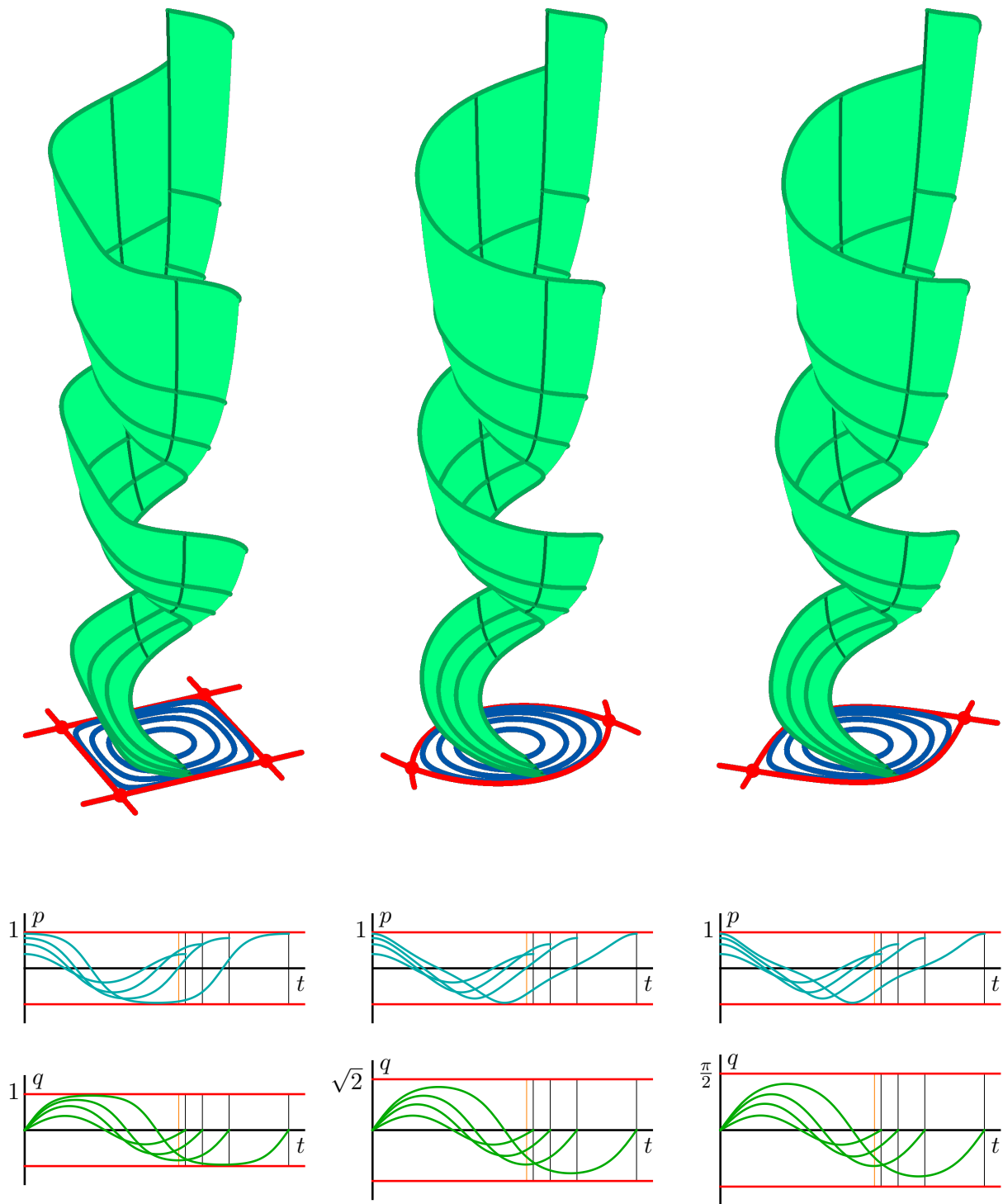


FIG. 14. Hamiltonian Flows and Their Vertical Projections Over One Period.

V. CONCLUSION

Hamiltonian mechanics teaches us to appreciate the truth and the beauty of classical mechanics through geometric abstractions such as phase portraits, energy landscapes, and time-evolving flows. Even more impressive, insightful geometry arises when incorporating complex time. The value inherent to one particular solution or sculptural model only increases through real and complex transformation theory, which enables proliferation of equivalent forms. In mathematics and physics, choice of coordinates always matters, as we have seen yet again in this problem about the simple pendulum. Coordinate transformation enables rapid analysis of period integrals in terms of an ordinary differential equation paired with coordinate-dependent certificate functions. A wide variety of oscillation disks will succumb to similar integral-differential analysis, so it is well-worth learning at the start.

Anharmonic period integrals have long been a topic of interest, not only for theorists, but also for experimental scientists. The days of Kepler and Galileo are receding ever farther into the past, and with them the frustrations of slow progress and low-precision measurement. Recent digital technologies—including slow-motion video and image processing—potentially enable the commonplace citizen scientist to begin measuring oscillation disks and period functions. Non-linearity presents a serious challenge to most student analysts, as they are over-accustomed to the status quo of linear experiments and linear regressions. In a planned followup article, we will actively address this weakness. The next article will describe an easily-reproducible, high-precision pendulum experiment, and will use the techniques of phase plane geometry to extract a shape parameter, which describes the similarity of the actual period function to its predicted form $4K(\alpha)$.

The harmonic hyperboloid and the anharmonic tori are only the first few examples on a magnificent bridge between physics and mathematics. The dream of "Hamilton-Abel" theory is to see more pedestrian and commercial traffic crossing this bridge. The simple pendulum affords one opportunity to exchange valuable ideas, but certainly, more opportunity abounds. An exciting frontier grows out of quantum Hamiltonian mechanics, and the sort of semiclassical calculations that owe back to the days of Ehrenfest and Sommerfeld. When we finally get to calculating complex-time tunneling integrals, Abel's original insight will seem all the more profound and prescient.

-
- [1] R.P. Feynman, R.B. Leighton, and M.L. Sands. *The Feynman Lectures on Physics*. Addison-Wesley, 1963.
- [2] Steven Strogatz. *Infinite Powers: How Calculus Reveals the Secrets of the Universe*. Houghton Mifflin Harcourt, 2019.
- [3] Mathematical Association of America. Euler archives, 2019. URL <http://eulerarchive.maa.org/>.
- [4] Jacques Dutka. The early history of the hypergeometric function. *Archive for History of Exact Sciences*, 31(1):15–34, 1984.
- [5] Maxim Kontsevich and Don Zagier. Periods. In *Mathematics unlimited—2001 and beyond*, pages 771–808. Springer, 2001.
- [6] D.E. Graham, R.L.; Knuth and O. Patashnik. *Concrete Mathematics: A Foundation for Computer Science*. Addison-Wesley, 1994.
- [7] Patrick Popescu-Pampu. *What is the Genus?* Springer, 2016.
- [8] David D. Nolte. The tangled tale of phase space. *Physics today*, 63(4):33–38, 2010.
- [9] A. Sommerfeld. *Atombau und Spektrallinien*. F. Vieweg & Sohn, 1921.
- [10] Eric J. Heller. *The Semiclassical Way to Dynamics and Spectroscopy*. Princeton University Press, 2018.
- [11] Steven Strogatz. *Nonlinear Dynamics and Chaos: With Applications to Physics, Biology, Chemistry, and Engineering*. CRC Press, 2018.
- [12] William G. Harter. *Classical Mechanics with a Bang!* University of Arkansas, 2019.
- [13] Harold Edwards. A normal form for elliptic curves. *Bulletin of the American mathematical society*, 44(3):393–422, 2007.
- [14] D. Bernstein and T. Lange. ECChacks: A gentle introduction to elliptic-curve cryptography, 2014. URL https://media.ccc.de/v/31c3_-_6369_-_en_-_saal_1_-_201412272145_-_ecchacks_-_djb_-_tanja_lange.
- [15] L.D. Landau and E.M. Lifshitz. *Mechanics*. Elsevier Science, 1982.
- [16] N.J.A. Sloane et al. Online Encyclopedia of Integer Sequences, 2019. URL <https://oeis.org>.

- [17] J. Gray. *Linear Differential Equations and Group Theory from Riemann to Poincare*. Modern Birkhäuser Classics. Birkhäuser Boston, 2010.
- [18] E.T. Whittaker and G.N. Watson. *A Course of Modern Analysis*. Cambridge University Press, 1902.
- [19] E.T. Whittaker. *A Treatise on the Analytical Dynamics of Particles and Rigid Bodies*. Cambridge University Press, 1904.